

Carter-Penrose diagrams for emergent spacetime in axisymmetrically accreting black hole systems

Susovan Maity,^{1,*} Md Arif Shaikh,^{2,†} Pratik Tarafdar,^{3,‡} and Tapas Kumar Das^{1,§}

¹*Harish-Chandra Research Institute, HBNI, Chhatnag Road, Jhansi, Allahabad 211 019, India*

²*International Centre for Theoretical Sciences, Tata Institute of Fundamental Research, Bangalore 560089, India*

³*The Institute of Mathematical Sciences, HBNI, IV Cross Road,
CIT Campus, Taramani, Chennai 600 113, India*

(Dated: June 16, 2021)

For general relativistic, inviscid, axisymmetric flow around Kerr black hole, one may choose different flow thickness. The stationary flow equations can be solved using methods of dynamical system to get transonic accretion flows, i.e, flow infalling in the black hole that turns supersonic from subsonic with decreasing radial distance, or vice versa. These transonic flows are obtained by choosing the particular flow passing through critical points of the phase portrait. For certain flow thickness like the one maintaining conical shape, the sonic point coincides with the critical point. But there are certain flows maintaining hydrostatic equilibrium, such as the one described by Novikov-Thorne, where the sonic point is not the same as the critical point. We perturb the flow for both kind of flow and study the behaviour of linear perturbation which behaves like a massless scalar field in some curved spacetime, known as analogue space-time. We draw the compactified causal structure, i.e, Penrose Carter diagram for both kind of analogue metric and prove that for both cases critical points are the acoustic horizons, whereas in the case where sonic points do not coincide with critical points, the sonic points are not the acoustic horizon, as one may expect from the definition of sound speed.

I. INTRODUCTION

For low angular momentum axially symmetric accretion flow around a rotating (Kerr) black hole, the accretion disc may have different disc geometry [1–5]. For discs with conical cross-section, the flow becomes transonic at the critical point, i.e, the Mach number becomes unity at the critical point itself. But for flow maintained in hydrostatic equilibrium, the Mach number does not become unity at the critical point.

Thus if one wants to use this stationary fluid flow as the background to analyse the behaviour of linear perturbation on it, then for certain cases the perturbation may obey the propagation equation of massless scalar field where we get an analogue metric dependent on the background flow variable [4–15]. In this case one must ask about the nature of acoustic horizon in this metric. From the definition of the sonic point, one may expect that the acoustic horizon should always coincide with it. But the dilemma of sonic point not coinciding with the critical point for discs in hydrostatic equilibrium is the main reason why one must investigate further and compare the case with that of the conical disc flow.

In this literature, we show that for conical flow, critical points are the same as the sonic points whereas the sonic points do coincide with the critical points for flow in hydrostatic equilibrium. There may be more than one sonic points present in the flow if the accretion disc is

endowed with a thin shock [2, 8, 16–39]. We construct the phase portrait corresponding to transonic integral solutions and choose a particular flowline such that shock arises in the flow and we get multitransonicity. Then in the next section, we linearly perturb the flows to show that the perturbations indeed follow the massless scalar field equation for our chosen models and obtain the analogue metric.

Then in the next section, we formulate the method for constructing the Penrose-Carter diagram which is compactified causal structure of the analogue metric. Then we show that sonic points are not the acoustic horizon as one may anticipate. Rather the critical points are more fundamental features of the flows which are the acoustic horizons. In the process, we also establish the thin shock as a white hole.

II. GOVERNING EQUATIONS AND CHOICE OF THE FLOW THICKNESS

We consider low angular momentum, inviscid, axially symmetric, irrotational accretion flow around a Kerr black hole. The background metric and fluid equations are the same for both the models we are considering. The difference arises from the height recipes we consider where one disc has a conical cross-section, i.e, the height linearly rise with the radial distance and the other one is in hydrostatic equilibrium. Below the details of the models are specified before the nature of critical points and further analysis by causal structure analysis of emergent acoustic metrics are carried out.

* susovanmaity@hri.res.in

† arif.shaikh@icts.res.in

‡ pratikt@imsc.res.in

§ tapas@hri.res.in

A. Background metric of Kerr black hole:

The background spacetime metric at its equatorial plane is given by

$$ds^2 = -\frac{r^2 \Delta}{A} dt^2 + \frac{r^2}{\Delta} dr^2 + \frac{A}{r^2} (d\phi - \omega dt)^2 + dz^2 \quad (1)$$

in Boyer-Lindquist coordinates, where

$$\Delta = r^2 - 2r + a^2, \quad A = r^2 + r^2 a^2 + 2ra^2, \quad \omega = \frac{2ar}{A}. \quad (2)$$

Here $a = \frac{J}{M}$ is the Kerr parameter. The metric mentioned above is obtained by using vertical averaging described in [40]. The physical horizon of Kerr black r_+ needed for analysing dynamics outside the physical black hole is given by

$$r_+ = 1 + \sqrt{1 - a^2} \quad (3)$$

in $G = 1, c = 1, M = 1$ unit.

B. The Euler and the continuity equations

The energy momentum tensor for a perfect fluid is given by

$$T^{\mu\nu} = (p + \epsilon)v^\mu v^\nu + pg^{\mu\nu}, \quad (4)$$

where ρ is the rest-mass energy density of the fluid, so that $\epsilon = \rho + \epsilon_{\text{thermal}}$. v^μ is the four-velocity with the normalization condition $v^\mu v_\mu = -1$.

Here we would like to clarify the velocity and other quantities that will be used throughout this paper. v^μ denotes the four-velocity in the Boyer-Lindquist frame, u denotes advective velocity, which is the three-component velocity in the co-rotating frame[41]. We will frequently denote v_0^μ , u_0 of four-velocity and advective velocity for the steady-state flow. In general, we will use the subscript zero to denote the value of physical variable corresponding to the stationary solutions of the steady flow, e.g., p_0, ρ_0 etc.

In the present work, we concentrate on the polytropic accretion only. The equation of state for adiabatic flow is given by $p = k\rho^\gamma$ where γ is the polytropic index and k is constant. Whereas for isothermal case $p \propto \rho$. The sound speed for adiabatic flow (isoentropic flow) is given by

$$c_s^2 = \left. \frac{\partial p}{\partial \epsilon} \right|_{\text{entropy}} = \frac{\rho}{h} \frac{\partial h}{\partial \rho}, \quad (5)$$

where h is the enthalpy given by

$$h = \frac{p + \epsilon}{\rho} \quad (6)$$

The continuity equation and the Euler equation are given by, respectively,

$$\nabla_\mu (\rho v^\mu) = 0 \quad (7)$$

and

$$\nabla_\mu T^{\mu\nu} = 0. \quad (8)$$

The Euler equation simplifies as

$$v^\mu \nabla_\mu v^\nu + \frac{c_s^2}{\rho} (v^\mu v^\nu + g^{\mu\nu}) \partial_\mu \rho = 0 \quad (9)$$

where expression of c_s^2 is used given by equation (5).

C. Choice of disc height

To obtain transonic flow one needs to choose flows that pass through critical points of the phase portrait of u vs r , even though the critical point may not be the sonic point for certain models. The exact method of obtaining the phase portrait and choosing flow through critical point will be demonstrated in the next section. But the key point concerning the critical point which differentiates the causal structure of our two chosen disc heights is as follows.

In simplistic accretion disc structure like constant height disc, i.e., where $H(r) = \text{constant}$ or conical disc, i.e., where $H(r)$ is a linear function of radial distance, has the common feature that the critical point turns out to be also the point where advective velocity is equal to sound speed as defined in , namely transonic points. But as will be derived, there are certain models for accretion disc around Kerr black hole in hydrostatic equilibrium for which the critical points and the transonic points do not coincide. Thus to point out the difference in Penrose-Carter Diagram, i.e., in the causal structures we may choose only two models. In one of them, the transonic point coincides with certain critical points. We choose conical flow for this purpose whose height function is given by

$$H_{CF}(r) = \Theta r \quad (10)$$

where Θ is the angular span of the conical structure. The oldest, and most used expression for the disc thickness for accretion flow maintained in the hydrostatic equilibrium along the vertical direction, was provided by Novikov & Thorne [42] as

$$H_{NT}(r) = \left(\frac{p}{\rho}\right)^{\frac{1}{2}} \frac{r^3 + a^2 r + 2a^2}{r^{\frac{3}{2}} + a} \sqrt{\frac{r^6 - 3r^5 + 2ar^{\frac{9}{2}}}{(r^2 - 2r + a^2)(r^4 + 4a^2 r^2 - 4a^2 r + 3a^4)}} \quad (11)$$

It is to be noted that accretion flow described by the above disc thickness can not be extended upto r_+ . The flow will be truncated at a distance r_T , where

$$(r_T)^{\frac{1}{2}} (r_T - 3) = 2a \quad (12)$$

which is outside r_+ . In reality of course the flow will exist upto r_+ but no stationary integral flow solutions can be constructed upto the close proximity of r_+ for accretion flow described by the Novikov-Thorne kind of disc heights.

Riffert and Herold [43] provided an expression of disc thickness by modifying the gravity-pressure balance condition of the treatment done in Novikov & Thorne as

$$H_{RH}(r) = \left(\frac{p}{\rho}\right)^{\frac{1}{2}} \sqrt{\frac{r^5 - 3r^4 + 2ar^{\frac{7}{2}}}{r^2 - 4ar^{\frac{1}{2}} + 3ar^2}} \quad (13)$$

Here the flow is also truncated at r_T as given by (12). Thus we see both the disc heights can be expressed in the form by $H(r) = \left(\frac{p}{\rho}\right)^{\frac{1}{2}} f(r, a)$. As will be seen later, this particular form of both the disc heights given by eq. (11) and eq. (13) is responsible for the fact that critical points do not coincide with the transonic points.

Abramowicz, Lanza and Percival [44] introduced an expression for the disc thickness, given by

$$H_{ALP}(r) = \left(\frac{p}{\rho}\right)^{\frac{1}{2}} \sqrt{\frac{2r^4}{v_\phi^2 - a^2(v_t - 1)}}, \quad (14)$$

for which the steady state accretion solutions can be obtained upto r_+ . Here v_ϕ and v_t are the azimuthal and time component of the four velocity of accreting fluid. It is, however to be noted that linear perturbation of the flow equation for flow thickness (14), it has not been possible to construct the acoustic metric till now.

In our present work, we thus use the height function due to Novikov & Thorne only as a representative of models where critical points are not transonic points.

III. NATURE OF CRITICAL POINTS FROM THE GROUND STATE SOLUTIONS

To find the critical points of the accretion flows, one needs the expression of the gradient of the advective velocity u_0 , i.e., the expression of du_0/dr for stationary accretion flow. To do that, two first integrals of motion for the stationary flow are needed. We first deal with the Euler equation as the height recipe does not enter in the equation. Then we differentiate between the conical flow and Novikov-Thorne type disc when we deal with the continuity equation.

In order to find out the first integral of motion in terms of advective velocity, we use the expression of v_0^r and v_{0t} in terms of u_0 . these relations are given by

$$v_0^r = \frac{u_0}{\sqrt{g_{rr}(1 - u_0^2)}} = \frac{\sqrt{\Delta} u_0}{r \sqrt{1 - u_0^2}} \quad (15)$$

and

$$v_{0t} = \sqrt{\frac{\Delta}{B(1 - u_0^2)}}. \quad (16)$$

The first integral of motion obtained by integrating the Euler equation is \mathcal{E}_0 and the second one obtained by integrating continuity equation is $\dot{\Xi}$.

The expression for derivative of advective velocity u_0 corresponding to the height function given by Eq. (10) turns out to be

$$\left. \frac{du_0}{dr} \right|_{CF} = \frac{u_0(1 - u_0^2) \left[c_{s0}^2 \frac{2r^2 - 3r + a^2}{\Delta r} + \frac{1}{2} \left(\frac{B'}{B} - \frac{\Delta'}{\Delta} \right) \right]}{u_0^2 - c_{s0}^2} = \frac{N_{CF}}{D_{CF}} \quad (17)$$

The expression for height function given by Eq. (11)

is (see [40])

$$\left. \frac{du_0}{dr} \right|_{NT} = \frac{u_0(1 - u_0^2) \left[\frac{2}{\gamma+1} c_{s0}^2 \left(\frac{\Delta'}{2\Delta} + \frac{f'}{f} \right) + \frac{1}{2} \left(\frac{B'}{B} - \frac{\Delta'}{\Delta} \right) \right]}{u_0^2 - \frac{c_{s0}^2}{\left(\frac{\gamma+1}{2}\right)}} = \frac{N_{NT}}{D_{NT}} \quad (18)$$

If we in general denote the numerator as N and denominator as D , then some parameter τ can be defined such that $\partial u_0/\partial\tau = N, \partial r/\partial\tau = D$

Thus the critical points are obtained from the condition $N = 0$ and $D = 0$.

Thus for conical flow, the condition at critical point is

$$u_0^2|_c = c_{s0}^2 \quad (19)$$

whereas for flow following the prescription of NT the condition will be

$$u_0^2|_c = c_{s0}^2|_c / \left(\frac{\gamma+1}{2}\right) \quad (20)$$

or for later convenience we can write

$$u_0^2|_c = \frac{c_{s0}^2|_c}{1+\beta}, \quad \text{where } \beta = \frac{\gamma-1}{2}. \quad (21)$$

The key point we get from eq. (19) and eq. (20) is that whereas the critical point is the transonic point in the case of Conical Flow, for NT disc height expression, the value of advective velocity is not the same as the sound speed at the critical point, i.e, the transonic and critical points are not same for flow with NT disc height.

One can simply assert that the fact that the critical point and transonic point do not coincide, is just a feature of the NT height function. But one may try to perturb the dynamical equations governing the flow and try to find out how linear perturbation behaves. The systematic analysis of perturbations of fluid equations leads to treating the linear perturbation in the context of analogue or emergent gravity. The perturbation of the flow will be done in the next section. But before that, we must present the critical or transonic flows in the phase portrait. The detailed derivation of the phase portrait corresponding to conical flow has been derived in and the derivation for NT disc height has been shown in. Below we just present the phase portrait and choose the flow on which we will perturb. We also show shock to be present in the flow such that there may be a discontinuous jump from the supersonic inner part of the accretion branch through the outer critical point to the subsonic outer part of the accretion branch through the inner critical point. The detailed analysis of shock in the ground state flow can be again found in [5].

In Fig. 1, phase portraits for conical flow and Novikov-Thorne are presented for the parameter value of $a = 0.40, \mathcal{E}_0 = 1.0012, \gamma = 1.35, \lambda = 3.0$, where the outermost r_{out} and innermost r_{in} critical points for both models are saddle-type in nature, whereas, the middle ones are center type in nature. We draw the phase portraits of Mach number (M) vs radial distance (r). Now we will choose a particular flow line from the phase portraits so that multi-transonic is achieved. This choice of multi-transonicity will give rise to interesting analogue space-time as will be seen later in the next part of the paper. The flow of a fluid element through this flow line we choose will be as follows.

The fluid elements in the disc accretion flows in hydrostatic equilibrium start far away from the gravitating body, in this case, the black hole, along the critical flow line and move through the outer critical point r_{out} , continue along the flow-line (the blue line in the online version of the figure) and will be supersonic till the flow variables and thermodynamic variables make a discontinuous jump to another branch (the green line in the online version of the figure) as a consequence of shock. The discontinuous jump occurs at S_1 in the blue flow line and reaches S_2 in the green flow line, where the flow becomes subsonic again, then the fluid element eventually goes through r_{in} . In this way the presence of shock makes the fluid element move through a flow line which is multi-transonic and a subset of the whole critical flow lines.

The major difference between conical flow and NT disc height is that whereas the flow achieves transonicity at r_{out} and again at r_{in} for conical flow, the flow for NT disc height does not, as the Mach number is lesser than 1 at r_{out} and r_{in} . For NT, the transonicity is first achieved at M_1 and for the second time after the shock, at M_2 .

This is the complete description of the stationary flow and the problem of non-coincidence of critical and sonic points for NT heights is evident. Now we need to study the behaviour of linear perturbations for these models to see how the causal structure of the emergent space-time corresponding to conical flow looks in a compactified form and to understand whether the nature of critical points can be clarified.

IV. DERIVATION OF ACOUSTIC METRIC FROM LINEAR PERTURBATION OF FLUID EQUATIONS

Now the perturbation on the stationary flow is done by following standard linear perturbation analysis [10, 11, 45, 46] where acoustic space-time metric for conical flow was derived. Time-dependent accretion variables, like the components of four velocity and pressure are written as small time-dependent linear perturbations added their stationary values. Thus we can write,

$$\begin{aligned} v^t(r, t) &= v_0^t(r) + v_1^t(r, t) \\ v^r(r, t) &= v_0^r(r) + v_1^r(r, t) \\ \rho(r, t) &= \rho_0(r) + \rho_1(r, t) \end{aligned} \quad (22)$$

where the subscript ‘1’ denotes the small perturbations of some variable about the stationary value denoted by subscript ‘0’. Now we denote \mathcal{M} as

$$\Psi = 4\pi\sqrt{-g}\rho(r, t)v^r(r, t)H_\theta \quad (23)$$

which is the stationary mass accretion rate of the accretion flow. Thus

$$\Psi(r, t) = \Psi_0 + \Psi_1(r, t) \quad (24)$$

Where Ψ_0 is the stationary mass accretion rate defined in equation (23). The constants can be absorbed in the

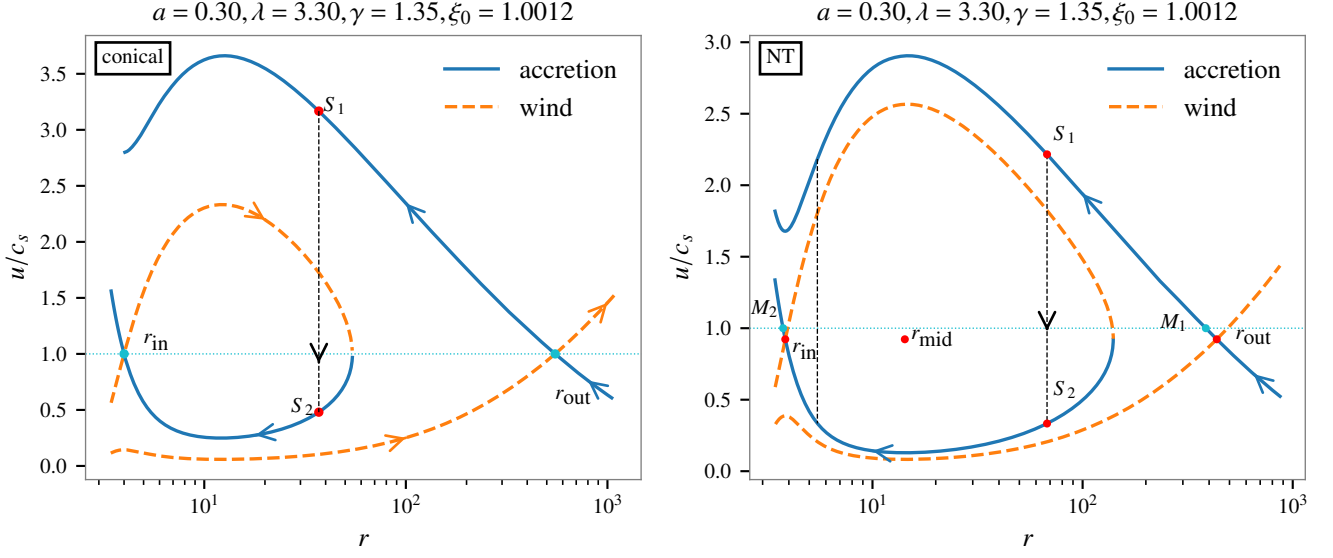


FIG. 1. *left*: Phase Portrait for Conical Flow. *right*: Phase Portrait for NT disc at $\mathcal{E}_0 = 1.0012$, $\lambda = 3.0$ and $\gamma = 1.35$ in monotonersonic case

definition without any loss of generality. Using the equations (22) we get

$$\Psi_1 = \sqrt{-g}[\rho_1 v_0^r H_{\theta 0} + \rho_0 v_1^r H_{\theta 0} + \rho_0 v_0^r H_{\theta 1}] \quad (25)$$

The last term in the perturbation Ψ_1 consists of a term with the perturbation of angular height function H_θ . We recall $H(r)$ as $H_\theta = H(r)/r$. For now, general height function $H(r)$ is used whereas later on we distinguish between conical flow and NT height.

For adiabatic flow (6) can be rewritten as

$$h = 1 + \frac{\gamma}{\gamma - 1} \frac{p}{\rho} \quad (26)$$

where the perturbed quantity h_1 can be written as

$$h_1 = \frac{h_0 c_{s0}^2}{\rho_0} \rho_1 \quad (27)$$

For adiabatic flow the irrotationality condition is [47]

$$\partial_\mu(hv_\nu) - \partial_\nu(hv_\mu) = 0 \quad (28)$$

Now, using (Eq. (28)), the normalization condition $v^\mu v_\mu = -1$ and the axis symmetry of the flow we obtain quantities needed for further perturbation. From irrotationality condition Eq. (28) with $\mu = t$ and $\nu = \phi$ and with axial symmetry we have

$$\partial_t(hv_\phi) = 0, \quad (29)$$

and for $\mu = r$ and $\nu = \phi$ and using axial symmetry, we have

$$\partial_r(hv_\phi) = 0. \quad (30)$$

So hv_ϕ is a constant of motion and eqn. (29) gives

$$\partial_t v_\phi = -\frac{v_\phi c_s^2}{\rho} \partial_t \rho. \quad (31)$$

Using $v_\phi = g_{\phi\phi} v^\phi + g_{\phi t} v^t$ in the previous equation gives

$$\partial_t v^\phi = -\frac{g_{\phi t}}{g_{\phi\phi}} \partial_t v^t - \frac{v_\phi c_s^2}{g_{\phi\phi} \rho} \partial_t \rho. \quad (32)$$

The normalization condition of four velocity $v^\mu v_\mu = -1$ in this case can be written as

$$g_{tt}(v^t)^2 = 1 + g_{rr}(v^r)^2 + g_{\phi\phi}(v^\phi)^2 + 2g_{\phi t}v^\phi v^t. \quad (33)$$

The time derivative of this equation is

$$\partial_t v^t = \alpha_1 \partial_t v^r + \alpha_2 \partial_t v^\phi \quad (34)$$

where $\alpha_1 = -v_r/v_t$, $\alpha_2 = -v_\phi/v_t$ and $v_t = -g_{tt}v^t + g_{\phi t}v^\phi$. Replacing $\partial_t v^\phi$ in Eq. (34) using Eq. (32) we get

$$\partial_t v^t = \left(\frac{-\alpha_2 v_\phi c_s^2 / (\rho g_{\phi\phi})}{1 + \alpha_2 g_{\phi t} / g_{\phi\phi}} \right) \partial_t \rho + \left(\frac{\alpha_1}{1 + \alpha_2 g_{\phi t} / g_{\phi\phi}} \right) \partial_t v^r \quad (35)$$

Using Eq. (22) in Eq. (35) and collecting the linear perturbation part we get

$$\partial_t v_1^t = \eta_1 \partial_t \rho_1 + \eta_2 \partial_t v_1^r \quad (36)$$

where

$$\eta_1 = -\frac{c_{s0}^2}{\Lambda v_0^t \rho_0} [\Lambda (v_0^t)^2 - 1 - g_{rr} (v_0^r)^2], \quad \eta_2 = \frac{g_{rr} v_0^r}{\Lambda v_0^t} \quad \text{and} \quad \Lambda = g_{tt} + \frac{g_{\phi t}^2}{g_{\phi\phi}} \quad (37)$$

Now we perturb height function and differentiate between the two models we consider. For conical flow, $H^{CF} = \Theta r$. Thus

$$H_{\theta 1}^{CF} = 0 \quad (38)$$

For NT, $H_{\theta 1}^{NT}$ can be written as

$$\frac{H_{\theta 1}^{NT}}{H_{\theta 0}^{NT}} = \left(\frac{\gamma - 1}{2} \right) \frac{\rho_1}{\rho_0} = \beta_{NT} \frac{\rho_1}{\rho_0} \quad (39)$$

where $\beta_{NT} = \frac{\gamma - 1}{2}$. Here we see that the whole perturbation analysis can be generalized if we define $\beta_{CF} = 0$ and continue the analysis with β in general. In the end we can again put these two different values and obtain different results for the two models.

The continuity equation takes the form

$$\partial_t (\sqrt{-g} \rho v^t H_\theta) + \partial_r (\sqrt{-g} \rho v^r H_\theta) = 0. \quad (40)$$

Using equation (22) and (24) in the previous equation and using equation (36) and (39) and replacing them in

(40) yields

$$-\frac{\partial_r \Psi_1}{\Psi_0} = \frac{\eta_2}{v_0^r} \partial_t v_1^r + \frac{v_0^t}{v_0^r \rho_0} \left[1 + \beta + \frac{\eta_1 \rho_0}{v_0^t} \right] \partial_t \rho_1, \quad (41)$$

and

$$\frac{\partial_t \Psi_1}{\Psi_0} = \frac{1}{v_0^r} \partial_t v_1^r + \frac{1 + \beta}{\rho_0} \partial_t \rho_1. \quad (42)$$

Using the two equations given by eq. (41) and (42) we can write $\partial_t v_1^r$ and $\partial_t \rho_1$ in terms of partial derivatives of Ψ_1 as

$$\begin{aligned} \partial_t v_1^r &= \frac{1}{\sqrt{-\tilde{g}} H_0 \rho_0 \tilde{\Lambda}} [(v_0^t (1 + \beta) + \rho_0 \eta_1) \partial_t \Psi_1 + (1 + \beta) v_0^r \partial_r \Psi_1] \\ \partial_t \rho_1 &= -\frac{1}{\sqrt{-\tilde{g}} H_0 \rho_0 \tilde{\Lambda}} [\rho_0 \eta_2 \partial_t \Psi_1 + \rho_0 \partial_r \Psi_1] \end{aligned} \quad (43)$$

where $\tilde{\Lambda}$ is given by

$$\tilde{\Lambda} = (1 + \beta) \left[\frac{g_{rr} (v_0^r)^2}{\Lambda v_0^t} - v_0^t \right] + \frac{c_{s0}^2}{\Lambda v_0^t} [\Lambda (v_0^t)^2 - 1 - g_{rr} (v_0^r)^2]. \quad (44)$$

Now we first linearly perturb Eq. (40) and then take it's time derivative, which in turn gives

$$\partial_t (h_0 g_{rr} \partial_t v_1^r) + \partial_t \left(\frac{h_0 g_{rr} c_{s0}^2 v_0^r}{\rho_0} \partial_t \rho_1 \right) - \partial_r (h_0 \partial_t v_{t1}) - \partial_r \left(\frac{h_0 v_{t0} c_{s0}^2}{\rho_0} \partial_t \rho_1 \right) = 0. \quad (45)$$

We can write

$$\partial_t v_{t1} = \tilde{\eta}_1 \partial_t \rho_1 + \tilde{\eta}_2 \partial_t v_1^r \quad (46)$$

with

$$\tilde{\eta}_1 = - \left(\Lambda \eta_1 + \frac{g_{\phi t} v_{\phi 0} c_{s0}^2}{g_{\phi\phi} \rho_0} \right), \quad \tilde{\eta}_2 = -\Lambda \eta_2. \quad (47)$$

Using eq. (46) in the Eq. (45) and dividing it by $h_0 v_{t0}$ yields

$$\partial_t \left(\frac{g_{rr}}{v_{t0}} \partial_t v_1^r \right) + \partial_t \left(\frac{g_{rr} c_s^2 v_0^r}{\rho_0 v_{t0}} \partial_t \rho_1 \right) - \partial_r \left(\frac{\tilde{\eta}_2}{v_{t0}} \partial_t v_1^r \right) - \partial_r \left(\left(\frac{\tilde{\eta}_1}{v_{t0}} + \frac{c_s^2}{\rho_0} \right) \partial_t \rho_1 \right) = 0 \quad (48)$$

where we use $h_0 v_{t0} = \text{constant}$. Finally replacing $\partial_t v_1^r$

and $\partial_t \rho_1$ in Eq. (48) using Eq. (43) one obtains

$$\begin{aligned} & \partial_t \left[k(r) \left(-g^{tt} + (v_0^t)^2 \left(1 - \frac{1+\beta}{c_s^2} \right) \right) \right] + \partial_t \left[k(r) \left(v_0^r v_0^t \left(1 - \frac{1+\beta}{c_s^2} \right) \right) \right] \\ & + \partial_r \left[k(r) \left(v_0^r v_0^t \left(1 - \frac{1+\beta}{c_s^2} \right) \right) \right] + \partial_r \left[k(r) \left(g^{rr} + (v_0^r)^2 \left(1 - \frac{1+\beta}{c_s^2} \right) \right) \right] = 0 \end{aligned} \quad (49)$$

where $k(r)$ is a conformal factor whose exact form is not required for the present analysis.

Eq. (49) can be written as

$$\partial_\mu (f^{\mu\nu} \partial_\nu \Psi_1) = 0 \quad (50)$$

where $f^{\mu\nu}$ is obtained from the symmetric matrix

$$f^{\mu\nu} = k(r) \begin{bmatrix} -g^{tt} + (v_0^t)^2 \left(1 - \frac{1+\beta}{c_s^2} \right) & v_0^r v_0^t \left(1 - \frac{1+\beta}{c_s^2} \right) \\ v_0^r v_0^t \left(1 - \frac{1+\beta}{c_s^2} \right) & g^{rr} + (v_0^r)^2 \left(1 - \frac{1+\beta}{c_s^2} \right) \end{bmatrix} \quad (51)$$

The equation (50) describes the propagation of the perturbation Ψ_1 in 1 + 1 dimension effectively. Equation (50) has the same form of a massless scalar field in curved spacetime (with metric $g^{\mu\nu}$) given by

$$\partial_\mu (\sqrt{-g} g^{\mu\nu} \partial_\nu \varphi) = 0 \quad (52)$$

where g is the determinant of the metric $g_{\mu\nu}$ and φ is the scalar field. Comparing equation (50) and (52), the acoustic spacetime $G_{\mu\nu}$ metric turns out to be

$$G_{\mu\nu}^{NT} = k_1(r) \begin{bmatrix} -g^{rr} - \left(1 - \frac{1+\beta}{c_{s0}^2} \right) (v_0^r)^2 & v_0^r v_0^t \left(1 - \frac{1+\beta}{c_{s0}^2} \right) \\ v_0^r v_0^t \left(1 - \frac{1+\beta}{c_{s0}^2} \right) & g^{tt} - \left(1 - \frac{1+\beta}{c_{s0}^2} \right) (v_0^t)^2 \end{bmatrix} \quad (53)$$

where $k_1(r)$ is also a conformal factor arising due to the process of inverting $G^{\mu\nu}$ in order to yield $G_{\mu\nu}$. For our present purpose we do not need the exact expression for $k_1(r)$. The suffix ‘NT’ is added because after the

derivation of this acoustic metric, it is convenient to use just one β and only NT has non-zero β .

Now one can put $\beta = 0$ to get the acoustic metric for conical flow which is

$$G_{\mu\nu}^{CF} = k_1(r) \begin{bmatrix} -g^{rr} - \left(1 - \frac{1}{c_{s0}^2} \right) (v_0^r)^2 & v_0^r v_0^t \left(1 - \frac{1}{c_{s0}^2} \right) \\ v_0^r v_0^t \left(1 - \frac{1}{c_{s0}^2} \right) & g^{tt} - \left(1 - \frac{1}{c_{s0}^2} \right) (v_0^t)^2 \end{bmatrix} \quad (54)$$

V. PENROSE CARTER DIAGRAM OF THE ACOUSTIC METRICS

From ground state solution of accretion flow, one expects the sonic point to be the acoustic horizon of the Analogue metric. But the non-trivial structure of the metric corresponding to NT height disc flow does not anymore assure that. Moreover, for both the metrics, the particular coordinate assures that setting $G^{rr} = 0$ will determine the condition at acoustic horizon. Thus we see that the condition at acoustic horizon for conical flow

will be obtained by putting $\beta = 0$ in eq. (51). This yields

$$g^{rr} + (v_0^r)^2 \left(1 - \frac{1}{c_s^2} \right) = 0 \quad (55)$$

which in turn yields $u_0 = c_{s0}$ at the acoustic horizon. But the condition at acoustic horizon for NT flow will be

$$g^{rr} + (v_0^r)^2 \left(1 - \frac{1+\beta}{c_s^2} \right) = 0 \quad (56)$$

which in turn yields $u_0 = \frac{c_{s0}}{\sqrt{1+\beta}}$ at the acoustic horizon. For later purpose it will be convenient to define an effective sound speed $c_{eff} = \frac{c_{s0}}{\sqrt{1+\beta}}$ for NT and $c_{eff} = c_{s0}$ for

conical flow.

One may formally analyze the causal structure of the acoustic space-time of the models to find the location of the horizon and also to understand the nature of acoustic horizon as they may represent physically different hypersurfaces with particular characteristics. In this section, we study the causal structure by using null coordinates and also construct the Penrose diagram of the acoustic metric. Penrose-Carter Diagram of analogue metric has been done by [48], but a simplistic constant sound speed was used and flow profiles were assumed instead of being derived from some fluid or any other underlying equations. In our analysis, the sound speed is a local variable of radial distance and obtained from fluid equations as shown earlier.

A. Acoustic Metric and Other Preliminaries

From the obtained acoustic metric the line element is given by

$$ds^2 = G_{tt}dt^2 + 2G_{tr}dtdr + G_{rr}dr^2. \quad (57)$$

where, the metric elements $G_{\mu\nu}$ are given by (54) and (53). The overall factor $k_1(r)$ is ignored as we want to finally focus on conformally transformed metric where this factor can be absorbed with the conformal factor.

Using eq. (15) and eq. (16) the metric elements of acoustic metrics turn out to be

$$\begin{aligned} G_{tt} &= \frac{u_0^2 - c_{\text{eff}}^2}{c_{\text{eff}}^2(1 - u_0^2)g_{rr}} \\ G_{tr} = G_{rt} &= \frac{u_0(1 - c_{\text{eff}}^2)F_1(r, \lambda)}{c_{\text{eff}}^2(1 - u_0^2)} \\ G_{rr} &= \frac{g_{rr}F_1^2(r, \lambda)(1 - c_{\text{eff}}^2)}{c_{\text{eff}}^2(1 - u_0^2)} - F_2(r) \end{aligned} \quad (58)$$

where

$$\begin{aligned} F_1(r, \lambda) &= \frac{g_{\phi\phi} + \lambda g_{\phi t}}{\sqrt{(g_{\phi\phi} + 2\lambda g_{\phi t} - \lambda^2 g_{tt})(g_{\phi\phi}g_{tt} + g_{\phi t}^2)g_{rr}}} \\ F_2(r) &= \frac{g_{\phi\phi}}{g_{\phi\phi}g_{tt} + g_{\phi t}^2} \end{aligned} \quad (59)$$

Thus we see that at a critical point where $u_0^2 = c_{\text{eff}}^2$, the metric element G_{tt} becomes zero. So we have to transform coordinate so that the co-ordinate singularity is removed. In the next section, we go through a systematic procedure such that the singularity is removed from new metric elements. Furthermore, we will conformally transform the final coordinates such that the infinite patch is mapped into a finite region of some coordinate space. This is helpful to study the causal structure of the acoustic metric by inspecting the Penrose-Carter Diagram.

B. Kruskal like Co-ordinate Transformation to Remove Singularity at Critical Point

First we choose null coordinates to write down the line element (57). We note that for null or lightlike curves $ds^2 = 0$, which yields

$$(dt - A_+(r)dr)(dt - A_-(r)dr) = 0 \quad (60)$$

where,

$$A_{\pm} = \frac{-G_{tr} \pm \sqrt{G_{tr}^2 - G_{rr}G_{tt}}}{G_{tt}}. \quad (61)$$

So instead of co-ordinates (t, r) , we choose new co-ordinates to be null co-ordinates (χ, ω) such that

$$d\omega = dt - A_+(r)dr \quad (62)$$

$$d\chi = dt - A_-(r)dr \quad (63)$$

Using coordinate transformation introduced in (62), the line element (57) can be written as

$$ds^2 = G_{tt}d\chi d\omega \quad (64)$$

After introducing the null coordinates, the next step usually should be affine parametrization, which removes the removable singularity. But one can remove the singularity of G_{tt} at the critical points by observing how the divergence behaves at the vicinity of horizon. To study this behaviour we expand $A_-(r)$ and $A_+(r)$ upto first order of $(r - r_c)$. Thus by expanding u_0 near r_c as

$$u_0(r) = -c_{\text{eff}}(r_c) + \left. \frac{du}{dr} \right|_{r_c} (r - r_c) + O((r - r_c)^2) \quad (65)$$

where the negative sign of the effective sound speed implies the flow is towards the origin. We also note that from (65), near r_c we can write

$$u_0^2 - c_{\text{eff}}^2 \approx -2 \left(c_{\text{eff}} \frac{du}{dr} \right)_{r_c} (r - r_c) \quad (66)$$

considering upto the first order term.

Now we expand $A_-(r)$ and $A_+(r)$ upto linear order of $(r - r_c)$. For that we first note that $G_{tt} \propto (u_0 - c_{\text{eff}})^2$ is very small near r_c which implies $|\frac{G_{tt}G_{rr}}{G_{tr}^2}| \ll 1$. Thus we obtain

$$A_+(r) = \frac{-G_{tr} + G_{tr} \left(1 - \frac{G_{tt}G_{rr}}{G_{tr}^2}\right)^{1/2}}{G_{tt}} \quad (67)$$

$$\approx -\frac{G_{rr}}{2G_{tr}} \quad (68)$$

and

$$A_-(r) = \frac{-G_{tr} - G_{tr} \left(1 - \frac{G_{tt}G_{rr}}{G_{tr}^2}\right)^{1/2}}{G_{tt}} \quad (69)$$

$$\approx -\frac{2G_{tr}}{G_{tt}} \quad (70)$$

$$= \frac{2F(r, \lambda)g_{rr}u_0(c_{\text{eff}}^2 - 1)}{u_0^2 - c_{\text{eff}}^2} \quad (71)$$

$$\approx \frac{F(r_c, \lambda)g_{rr}(u_{0c}^2 - 1)}{u'_{0c} - (c'_{\text{eff}})_c} \frac{1}{r - r_c} \quad (72)$$

$$= \frac{1}{\kappa} \frac{1}{r - r_c} \quad (73)$$

where

$$\kappa = \frac{u'_{0c} - (c'_{\text{eff}})_c}{F(r_c, \lambda)g_{rr}(u_{0c}^2 - 1)}. \quad (74)$$

So, we see that although

$$\chi \approx t - \frac{1}{\kappa} \ln|r - r_c| \quad (75)$$

shows a logarithmic divergence at $r \rightarrow r_c$, the form of G_{rr} and G_{tr} ensures that

$$\omega = t + \int \frac{G_{rr}}{2G_{tr}} dr \quad (76)$$

does not diverge at the critical point as the function inside integral is regular there.

Thus we see that near critical point

$$e^{-\kappa\chi} \propto e^{-\kappa t} |r - r_c| \propto e^{-\kappa t} (u_0^2 - c_{\text{eff}}^2) \quad (77)$$

Now one can compare the null co-ordinates in this case with that of the Schwarzschild metric and guess a co-ordinate transformation such that the singularity of metric element at critical point is removed. The transformation equations can be given by

$$\begin{aligned} U(\chi) &= -e^{-\kappa\chi} \\ W(\omega) &= e^{\kappa\omega} \end{aligned} \quad (78)$$

Using this new set of co-ordinates (U, W) , the line element can now be written as

$$ds^2 = G_{tt} \frac{e^{\kappa(\chi-\omega)}(u_0^2 - c_{\text{eff}}^2)}{\kappa^2 c_{\text{eff}}^2 (1 - u_0^2)(1 - 2/r + a/r^2)^{-1}} dU dW. \quad (79)$$

Thus at the numerator of the new metric element, the two factors multiplied together will cancel the divergence at the critical points. Thus these new co-ordinates (U, W) are similar to the Kruskal coordinates for the case of Schwarzschild metric which removes the co-ordinate singularity.

Now we have to compactify the infinite space into a finite patch of some coordinates. For that, the co-ordinates will be (T, R) such that

$$T = \frac{\tan^{-1}(W) + \tan^{-1}(U)}{2} \quad (80)$$

$$R = \frac{\tan^{-1}(W) - \tan^{-1}(U)}{2} \quad (81)$$

C. Penrose Carter Diagram

Now we have constructed the necessary transformations to draw the Penrose-Carter Diagrams for both conical flow and NT flow. The flow lines we chose previously was used as the background flow and the acoustic metric was formed numerically. Then by the prescribed transformations, Penrose Carter Diagram was obtained which is presented below where $r = \text{constant}$ lines are drawn. In Fig. 2, we draw the Penrose-Carter diagram for conical flow (left) and Novikov-Thorne model (right). There are four separate regions in the analogue spacetimes. let's denote the outer and inner critical points as r_{out} and r_{in} . The first squares (blue) on the right side is the region outside r_{out} . The second square (yellow) from right side is the region inside r_{out} and outside r_{shock} . The third square (green) from the right side represents the region between r_{shock} and r_{in} which is subsonic. The fourth region (red) is the leftmost triangular part of the diagram representing the interior of r_{in} . This region is another black hole where the boundary r_{in} acts as black hole horizon.

Now from the diagrams, the light cones are at 45° and 135° to the horizontal lines if the scale of both T and R is the same. The negative slope portion of the blue line at the extreme right belonging to the first region approximately gives the null infinity. Now, the formal definition of the black hole event horizon from the point of view of differential geometry, i.e., the event horizon is the boundary of the black hole region separating it from the Causal Past of Future Null infinity. Mathematically, this translates to

$$\mathfrak{H} = \partial BH \cap \partial J^- (\mathcal{I}^+). \quad (82)$$

Thus from the definition of the horizon, we see that for each of the model, there are two horizons, one of which is the boundary of blue and yellow regions, i.e, the outer critical point r_{out} and the other one is the boundary of green and red regions, i.e, the inner critical point r_{in} . We also see that the boundary between yellow and green regions for both models, i.e, the point at which the thin shock occurs, act as a white whole for the green region.

In the case of PCD for conical flow, the boundary of the blue and yellow lines denote the critical or sonic points which are the same in this case. But for NT, we see that $r = \text{constant}$ lines corresponding to sonic point lies inside the second region and is denoted by a yellow line. Thus, in this case, the sonic point does not act as the deciding boundary of propagation for linear perturbation.

VI. CONCLUDING REMARKS

From the analysis of the ground state of stationary flow we got that whereas the sonic and critical points coincide for conical flow, the critical and sonic points do not coincide for a disc in hydrostatic equilibrium. The reason for this is that whereas the flow thickness for conical flow is

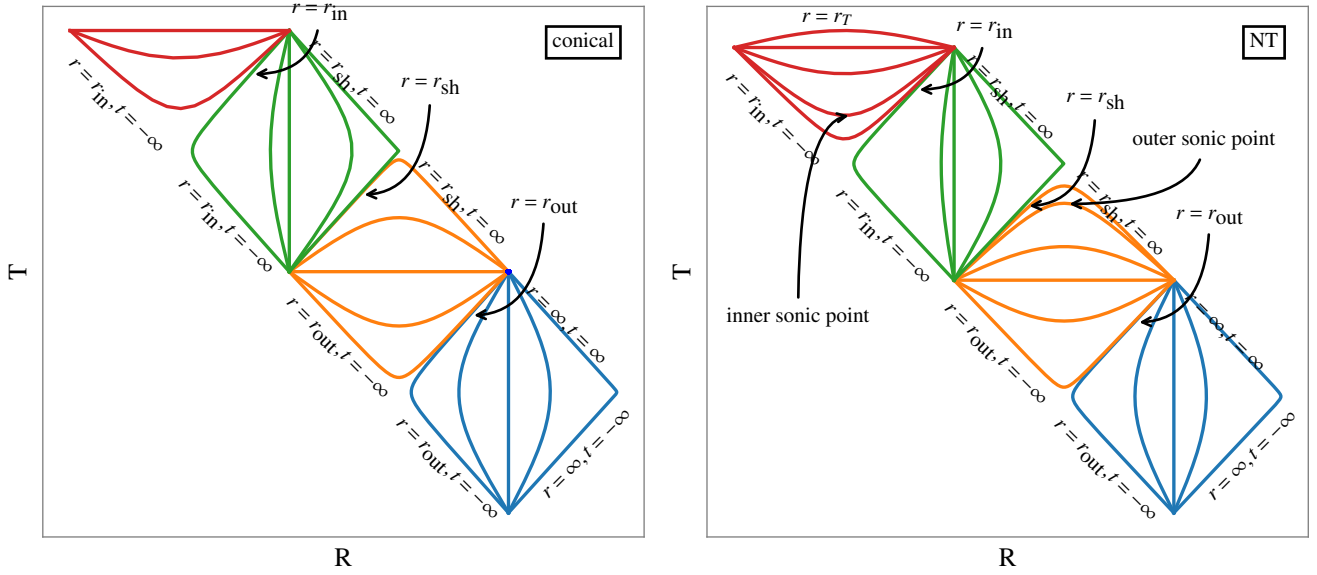


FIG. 2. *left*: Penrose-Carter diagram for conical flow. *right*: Penrose-Carter diagram for Novikov-Thorne model.

only geometry dependent, i.e., depends on radial distance only, the flow thickness we chose is also dependent on the local sound speed.

The causal structure analysis for both the flows shows that although one may assert that the perturbation should cross the sonic point from one direction only, that is not the case where the critical point is different from the sonic point. The role of this boundary, which is the acoustic horizons for the analogue metric followed by the

perturbed flow is fulfilled by the critical point.

Moreover one can see from both the Penrose-Carter Diagram that the thin shock which brings the flow discontinuously from one flow line to another acts as a white hole for the subsonic region between the inner critical point and the location of the shock.

This analysis is also the one where for the first time a numerical approach is proposed to draw Penrose Carter diagram for a variable sound speed, which is the consequence of choosing adiabatic flow.

-
- [1] S. K. Chakrabarti and S. Das, Model dependence of transonic properties of accretion flows around black holes, *Monthly Notices of the Royal Astronomical Society* **327**, 808 (2001).
- [2] M. A. Abramowicz and S. K. Chakrabarti, Standing shocks in adiabatic black hole accretion of rotating matter, *Astrophysical Journal* **350**, 281 (1990).
- [3] S. Nag, S. Acharya, A. K. Ray, and T. K. Das, The role of flow geometry in influencing the stability criteria for low angular momentum axisymmetric black hole accretion, *New Astronomy* **17**, 285 (2012).
- [4] P. Tarafdar and T. K. Das, Dependence of acoustic surface gravity on geometric configuration of matter for axially symmetric background flows in the schwarzschild metric, *International Journal of Modern Physics D* **24**, 1550096 (2015).
- [5] P. Tarafdar and T. K. Das, Influence of the geometric configuration of accretion flow on the black hole spin dependence of relativistic acoustic geometry, *International Journal of Modern Physics D* **27**, 1850023 (2018).
- [6] T. K. Das, Analogue hawking radiation from astrophysical black-hole accretion, *Classical and Quantum Gravity* **21**, 5253 (2004).
- [7] S. Dasgupta, N. Bilic, and T. K. Das, Pseudo-schwarzschild spherical accretion as a classical black hole analogue, *General Relativity and Gravitation* **37**, 1877 (2005).
- [8] T. K. Das, N. Bilić, and S. Dasgupta, A black-hole accretion disc as an analogue gravity model, *Journal of Cosmology and Astroparticle Physics* **2007** (06), 009.
- [9] S. Saha, S. Sen, S. Nag, S. Raychowdhury, and T. K. Das, Model dependence of the multi-transonic behaviour, stability properties and the corresponding acoustic geometry for accretion onto rotating black holes, *New Astronomy* **43**, 10 (2016).
- [10] M. A. Shaikh, I. Firdousi, and T. K. Das, Relativistic sonic geometry for isothermal accretion in the schwarzschild metric, *Classical and Quantum Gravity* **34**, 155008 (2017).
- [11] M. A. Shaikh, Relativistic sonic geometry for isothermal accretion in the kerr metric, *Classical and Quantum Gravity* **35**, 055002 (2018).
- [12] M. A. Shaikh and T. K. Das, Linear perturbations of low angular momentum accretion flow in the kerr metric and the corresponding emergent gravity phenomena, *Phys. Rev. D* **98**, 123022 (2018).
- [13] B. Muchotrzeb, Transonic accretion flow in a thin disk around a black hole. II, *Acta Astronomica* **33**, 79 (1983).

- [14] J. Fukue, Shock propagations in a geometrically thin accretion disk, *Publications of the Astronomical Society of Japan* **35**, 355 (1983).
- [15] J. Fukue, Transonic disk accretion revisited, *PASJ* **39**, 309 (1987).
- [16] S. Carroll, *Spacetime and Geometry: An Introduction to General Relativity* (Addison Wesley, 2004).
- [17] H. Abraham, N. Bilic, and T. K. Das, Acoustic horizons in axially symmetric relativistic accretion, *Classical and Quantum Gravity* **23**, 2371 (2006).
- [18] H.-Y. Pu, I. Maity, T. K. Das, and H.-K. Chang, On spin dependence of relativistic acoustic geometry, *Classical and Quantum Gravity* **29**, 245020 (2012).
- [19] J. F. Lu, Non-uniqueness of transonic solution for accretion onto a Schwarzschild black hole, *Astronomy and Astrophysics* **148**, 176 (1985).
- [20] J. F. Lu, Sound horizon of accretion onto a kerr black hole, *General Relativity and Gravitation* **18**, 45 (1986).
- [21] B. Muchotrzeb and C. B., *Acta Astronomica* **36** (1986).
- [22] M. A. Abramowicz and S. Kato, Constraints for transonic black hole accretion, *Astrophysical Journal* **336**, 304 (1989).
- [23] S. K. Chakrabarti, Standing Rankine-Hugoniot shocks in the hybrid model flows of the black hole accretion and winds, *Astrophysical Journal* **347**, 365 (1989).
- [24] S. K. Chakrabarti, Accretion processes on a black hole, *Physics Reports* **266**, 229 (1996).
- [25] M. Kafatos and R. X. Yang, Transonic Inviscid Disc Flows in the Schwarzschild Metric - Part One, *Monthly Notices of the Royal Astronomical Society* **268**, 925 (1994).
- [26] R. Yang and M. Kafatos, Shock study in fully relativistic isothermal flows, 2, *Astronomy and Astrophysics* **295**, 238 (1995).
- [27] V. I. Pariev, Hydrodynamic accretion on to a rapidly rotating kerr black hole, *Monthly Notices of the Royal Astronomical Society* **283**, 1264 (1996).
- [28] J. Peitz and S. Appl, Viscous accretion discs around rotating black holes, *Monthly Notices of the Royal Astronomical Society* **286**, 681 (1997).
- [29] D. M. Caditz and S. Tsuruta, Adiabatic shocks in accretion flows, *The Astrophysical Journal* **501**, 242 (1998).
- [30] T. K. Das, Generalized shock solutions for hydrodynamic black hole accretion, *The Astrophysical Journal* **577**, 880 (2002).
- [31] T. K. Das, J. K. Pendharkar, and S. Mitra, Multitransonic black hole accretion disks with isothermal standing shocks, *The Astrophysical Journal* **592**, 1078 (2003).
- [32] P. Barai, T. K. Das, and P. J. Wiita, The dependence of general relativistic accretion on black hole spin, *The Astrophysical Journal Letters* **613**, L49 (2004).
- [33] J. Fukue, Sound Speed and the Pseudo-Newtonian Potential, *Publications of the Astronomical Society of Japan* (2004).
- [34] T. Okuda, V. Teresi, E. Toscano, and D. Molteni, Radiative shocks in rotating accretion flows around black holes, *Publications of the Astronomical Society of Japan* **56**, 547 (2004).
- [35] T. Okuda, V. Teresi, and D. Molteni, Shock oscillation model for quasi-periodic oscillations in stellar mass and supermassive black holes, *Monthly Notices of the Royal Astronomical Society* **377**, 1431 (2007).
- [36] T. K. Das and B. Czerny, Hysteresis effects and diagnostics of the shock formation in low angular momentum axisymmetric accretion in the kerr metric, *New Astronomy* **17**, 254 (2012).
- [37] P. Suková and A. Janiuk, Shocks in the low angular momentum accretion flow, *Journal of Physics: Conference Series* **600**, 012012 (2015).
- [38] P. Suková and A. Janiuk, Oscillating shocks in the low angular momentum flows as a source of variability of accreting black holes, *Monthly Notices of the Royal Astronomical Society* **447**, 1565 (2015).
- [39] P. Suková, S. Charzyński, and A. Janiuk, Shocks in the relativistic transonic accretion with low angular momentum, *Monthly Notices of the Royal Astronomical Society* **472**, 4327 (2017).
- [40] P. Tarafdar, D. B. Ananda, S. Nag, and T. K. Das, Influence of matter geometry on shocked flows-ii: Accretion in the kerr metric, arXiv preprint arXiv:1612.06882 (2016).
- [41] See [49] for the detailed description of expressions in various velocities in different frames for accretion flow with angular momentum in Kerr metric.
- [42] I. D. Novikov and K. S. Thorne, Astrophysics of black holes., in *Black Holes (Les Astres Occlus)*, edited by C. Dewitt and B. S. Dewitt (1973) pp. 343–450.
- [43] H. Riffert and H. Herold, Relativistic Accretion Disk Structure Revisited, *The Astrophysical Journal* **450**, 508 (1995).
- [44] M. A. Abramowicz, A. Lanza, and M. J. Percival, Accretion disks around kerr black holes: Vertical equilibrium revisited, *The Astrophysical Journal* **479**, 179 (1997).
- [45] D. B. Ananda, S. Bhattacharya, and T. K. Das, Acoustic geometry through perturbation of mass accretion rate: radial flow in static spacetimes, *General Relativity and Gravitation* **47**, 96 (2015).
- [46] D. A. Bollimpalli, S. Bhattacharya, and T. K. Das, Perturbation of mass accretion rate, associated acoustic geometry and stability analysis, *New Astronomy* **51**, 153 (2017).
- [47] N. Bilic, Relativistic acoustic geometry, *Classical and Quantum Gravity* **16**, 3953 (1999).
- [48] C. Barceló, S. Liberati, S. Sonego, and M. Visser, Causal structure of analogue spacetimes, *New Journal of Physics* **6**, 186 (2004).
- [49] C. F. Gammie and R. Popham, Advection-dominated accretion flows in the kerr metric. i. basic equations, *The Astrophysical Journal* **498**, 313 (1998).